Synergistic combination of alkylphosphocholines with peptaibols in targeting *Leishmania infantum in vitro*

Irene Fragiadaki[a], Anna Katogiritis[a,1], Theodora Calogeropoulou[b], Hans Brückner[c], Effie Scoulica[a,*]

[a] *University of Crete, Department of Clinical Microbiology and Microbial Pathogenesis, Faculty of Medicine, P.O. Box 2208, Heraklion, Greece*
[b] *National Hellenic Research Foundation, Institute of Biology Medicinal Chemistry and Biotechnology, 48 Vassileos Constantinou Ave., 116 35, Athens, Greece*
[c] *Institute of Nutritional Sciences, Interdisciplinary Research Center (IFZ), University of Giessen, 35390, Giessen, Germany*

ARTICLE INFO

ABSTRACT

Anti-leishmanial treatment increasingly encounters therapeutic limitations due to drug toxicity and development of resistance. The effort for new therapeutic strategies led us to work on combinations of chemically different compounds that could yield enhanced leishmanicidal effect. Peptaibols are a special type of antimicrobial peptides that are able to form ion channels in cell membranes and potentially affect cell viability. We assayed the antileishmanial activity of two well studied helical peptaibols, the 16-residue antiamoebin and the 20-residue alamethicin-analogue suzukacillin, and we evaluated the biological effect of their combination with the alkyl-phosphocholine miltefosine and its synthetic analogue TC52. The peptaibols tested exhibited only moderate antileishmanial activity, however their combination with miltefosine had a super-additive effect against the intracellular parasite (combination index 0.83 and 0.43 for antiamoebin and suzukacillin respectively). Drug combinations altered the redox stage of promastigotes, rapidly dissipated mitochondrial membrane potential and induced concatenation of mitochondrial network promoting spheroidal morphology. These results evidenced a potent and specific antileishmanial effect of the peptaibols/miltefosine combinations, achieved with significantly lower concentrations of the compounds compared to monotherapy. Furthermore, they revealed the importance of exploring novel classes of bioactive compounds such as peptaibols and demonstrated for the first time that they can act in synergy with currently used antileishmanial drugs to improve the therapeutic outcome.

1. Introduction

Leishmaniases are devastating human diseases of grossly underestimated public health impact. They are endemic in 88 countries worldwide with an estimate of 2 million new cases occurring annually (1.5 million cases of cutaneous leishmaniasis and 500.000 of visceral leishmaniasis) and about 12 million people currently infected (Desjeux et al., 1991). The responsible pathogens for these diseases belong to genus *Leishmania* and are unicellular parasites with digenetic life cycles: the extracellularly living promastigote that develops in the sandfly vector, and the intracellular amastigote that resides in the mammalian host cells. Human leishmaniases can manifest as cutaneous (CL), mucocutaneous (MCL) or visceral (VL), the latter being the most life threatening form if left untreated (Chappuis et al., 2007; David and Craft, 2009). VL can cause large-scale and tenacious epidemics, with high case–fatality rates. Children under the age of 15 years are the most

severely affected group. Domestic dogs are the principal animal reservoir for the infection.

Although the *Leishmania* genome has been unraveled and the immunology of the disease is well characterized, an effective vaccine has not yet been discovered, rendering chemotherapy the only treatment. Besides the prohibitive cost for many endemic areas of the currently available drugs, their clinical efficacy is seriously jeopardized by severe side effects as well as the emergence of resistant parasites. All these factors point towards the necessity for the discovery of alternative treatments (Mishra et al., 2007).

The discovery of the antileishmanial activity of hexadecylphosphocholine (miltefosine, HePC), initially developed as an antitumor agent, constituted a major breakthrough in antileishmanial chemotherapy (Croft et al., 1987). HePC is effective against both VL and CL, is orally administered and displays good bioavailability (Croft et al., 2005; Croft, 2008). Moreover, it has been approved by the US FDA in

2014 for the treatment of all forms of the disease. The cell membrane appears to be the primary site of HePC activity, due to interference with lipid metabolism and lipid-dependent signal transduction (Lux et al., 1996; Lira et al., 2001; Dorlo et al., 2012). The mitochondrion of trypanosomatids is a possible target of lipid compounds that induce an impairment of the energy production and modulation of the redox stage of the cell (Santa-Rita et al., 2004; Murray et al., 2014).

However, despite its advantages, HePC has a long half-life (100–200 h) and a low therapeutic ratio in humans, characteristics that encourage development of resistance. Moreover, teratogenesis (Herwaldt, 1999) and diminished efficacy of the compound when administered to HIV-coinfected patients (Sindermann et al., 2004) or against the wide range of CL syndromes, are important issues that have to be addressed. Finally, the use of HePC against kala-azar in Europe, prognosticate an increase in resistance and rapid obsolescence of this drug (Berman et al., 2006). One potential source of new therapeutic agents is the vast and diverse biological repertoire of antimicrobial peptides (AMPs). These 10–50 residues-long polypeptides constitute essential components of the innate immune systems of organisms from all Kingdoms (Hancock and Diamond, 2000). Recently, AMPs were used in clinical trials for systemic as well as topical treatment of bacterial infections (Ashby et al., 2014). They have been also proved effective antileishmanial agents (Gaidukov et al., 2003; Guerrero et al., 2004; Mangoni et al., 2005). Unlike antibiotics which target specific cellular activities, AMPs target cell membranes by altering fluidity or compromising the bilayer integrity by forming channels and facilitating the flux of cellular constituents (Teixeira et al., 2012). However the vulnerability of these peptides to either host- or parasite-derived proteases, raised some concerns regarding their adequacy as antileishmanial drugs (Kulkarni et al., 2006).

Of medical interest in this fast-growing field are a group of non-ribosomally synthesized AMPs termed peptaibols, representing a subgroup of bioactive peptides termed comprehensively peptaibiotics (https://peptaibiotics-database.boku.ac.at/django). The majority comprises linear peptides of 15–20 residues, defined as *N*-acetylated **pep**tides containing **Aib** (α-aminoisobuyric acid; 2-methylalanine) and a C-terminal bound 1,2-amino alcoho**l** such as phenylalaninol. Due to their high content in sterically constrained Aib residues, they are incompatible as protease substrates (Bruckner et al., 1984). Peptaibols have attracted much attention due to their broad range of bioactivities which include growth inhibition of bacteria, fungi, protozoa and possibly helminthes (Szekeres et al., 2005). Furthermore, their insecticidal action on mosquito larvae has been reported (Matha et al., 1992).

The biological activity of peptaibols is attributed to their membrane modifying properties, and specifically to the formation of channels that result in leakage of cytoplasmic material, ultimately leading to cell death (Boheim, 1974; Balaram et al., 1992; Peltola et al., 2004; Shi et al., 2010). Furthermore, peptaibols seem to cause pathological changes to the ultrastructure of mitochondria (Reed and Lardy, 1975; Bruckner and Toniolo, 2013). It has been shown that the peptaibol AAM exhibits trypanocidal activity in a mouse model for trypanosomiasis (Kumar et al., 1991), effect attributed to the channel-forming capacity that dissipates the parasite mitochondrial membrane potential, or alters the parasite's plasma membrane integrity (Nagaraj et al., 2001).

In our previous studies on structure-activity relationships of alkylphospholipids we described miltefosine derivatives substituted by rings of various sizes in the lipid portion and/or the head group, which have exhibited improved antileishmanial activity and reduced toxicity with respect to the prototype approved drug HePC (Avlonitis et al., 2003; Calogeropoulou et al., 2008; Papanastasiou et al., 2010; Godinho et al., 2013).

In this report we describe the leishmanicidal effect of two peptaibols, antiamoebin (AAM) and suzukacillin (SZ). We determined their activity against the promastigote and intracellular amastigote form of the parasite as well as their cytotoxicity and hemolytic activity. We assessed their effect on the physiology of the mitochondrion in the promastigote by measuring Reactive Oxygen Species (ROS) production, mitochondrial membrane potential ($\Delta\Psi$m) alteration and recording morphological changes. Finally we evaluated the synergistic effect of combining suboptimal concentrations of these peptaibols with HePC, or with its less active synthetic triasolyl-substituted alkylphosphocholine (APC) analogue TC52, against the intracellular amastigote.

2. Materials and methods

2.1. Parasite and cell culture

A field strain of *L. infantum* was isolated from the spleen of an infected dog which was euthanized after advanced kala-azar disease diagnosis. Briefly, the spleen was cleaned by washing in sterile PBS (Invitrogen, Grand Island, NY, USA) and 70% ethanol (Sigma Aldrich Inc, St Louis, USA). Then a small piece was carefully dissected and homogenized in RPMI, supplemented with 10% FBS (decomplemented at 56 °C for 30 min) and 2% penicillin/streptomycin. The homogenized solution was placed in a Falcon flask (Nunc, Denmark, Roskild) and was incubated at 26 °C, until promastigotes of the parasite were visible. The human monocytic THP-1 cell line was also cultured in RPMI containing FBS and antibiotics as indicated above, and was maintained at 37 °C in a humidified atmosphere containing 5% CO_2. All cell culture media were obtained from Invitrogen and cell culture flasks and plates were purchased from Nunc and Costar (Cambridge, MA).

2.2. Ether phospholipids and peptides

HePC and the analogue TC52, a 1,2,3-triazolyl-substituted derivative ({2-[11-(4′-pentyl-(1′,2′,3′)triazol-1-yl)undecylphosphinyloxy]ethyl} N,N,N trimethylammonium inner salt) were synthesized in house (manuscript on synthesis and activity of the analogue, in preparation) (Fig. 1A). AAM was isolated from the fermentation broth of *Emericellopsis synnematicola* CBS 176.60 (Jaworski and Bruckner, 2000) and suzukacillin A (SZ-A) from *Trichoderma viride* C1 (Krause et al., 2006). Both peptides represent microheterogenous mixtures, distinguished by limited exchange of a single or few amino acids. However, major component of AAM preparation is antiamoebin I and of SZ-A is SZ-A4 (Fig. 1B). Stock solutions were prepared in DMSO (Sigma) and preserved at −20 °C.
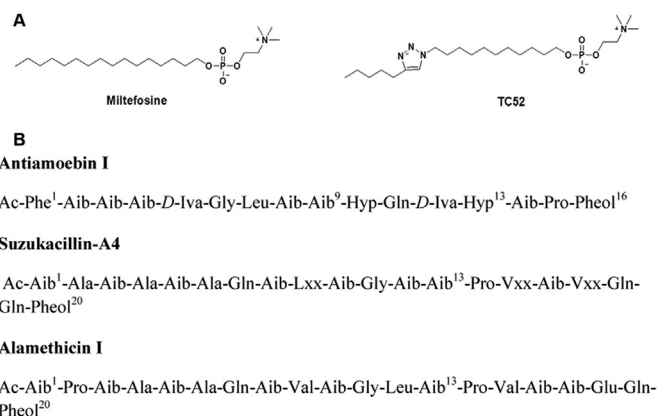

A

Miltefosine   TC52

B

Antiamoebin I

Ac-Phe[1]-Aib-Aib-Aib-*D*-Iva-Gly-Leu-Aib-Aib[9]-Hyp-Gln-*D*-Iva-Hyp[13]-Aib-Pro-Pheol[16]

Suzukacillin-A4

Ac-Aib[1]-Ala-Aib-Ala-Aib-Ala-Gln-Aib-Lxx-Aib-Gly-Aib-Aib[13]-Pro-Vxx-Aib-Vxx-Gln-Gln-Pheol[20]

Alamethicin I

Ac-Aib[1]-Pro-Aib-Ala-Aib-Ala-Gln-Aib-Val-Aib-Gly-Leu-Aib[13]-Pro-Val-Aib-Aib-Glu-Gln-Pheol[20]

Fig. 1. A. Chemical structures of Miltefosine and its analogue TC52. **B.** Sequences of AAM I (major sequence) and SZ-A4 in comparison to alamethicin I (= alamethicin F30/3). Abbreviations: Ac, acetyl; Phe, phenylalanine; Ala, alanine; Aib, α-aminoisobutyric acid (2-methylalanine); Iva, isovaline (2-ethylalanine); Gly, glycine; Lxx, leucine (Leu) or isoleucine (Ile); Vxx, valine (Val) or isovaline (Iva); Hyp, *trans*-4-hydroxyproline; Pro, proline; Gln, glutamine; Glu, glutamic acid; Pheol, L-phenylalaninol. Chiral amino acids and Pheol are of the L-configuration with the exception of *D*-Iva.

2.3. Biological evaluation of the compounds and their combinations

2.3.1. Determination of the antileishmanial activity in promastigote cultures

Promastigotes were incubated at a density of 10^6 parasites/ml with serial dilutions of the compounds for 24 h at 26 °C. Following incubation, promastigotes were harvested, resuspended in PBS, stained with 12 μM propidium iodide (PI) (Invitrogen) and analyzed by flow cytometry as described below. Each compound was assigned the IC_{50} value that represents the compound concentration that kills 50% of the parasite population. Calculation of IC_{50} values was carried out as described previously (Huber and Koella, 1993; Calogeropoulou et al., 2008).

2.3.2. Determination of antileishmanial activity against intracellular L.infantum

THP-1 cells were differentiated with 1 μM retinoic acid (Sigma) for 72 h at 37 °C/5% CO_2. Parasites were added at a cell:parasite ratio of 1:4, and allowed to infect macrophages overnight. To remove excess promastigotes, cells were pelleted by centrifugation, resuspended in RPMI and laid over Histopaque 1077 (Invitrogen). Following centrifugation at 1300g for 20 min, the cell layer containing the infected macrophages was collected, washed, and incubated with serial dilutions of the compounds and their combinations, for 24 h at 37 °C/5% CO_2. At the end of the experiment, 10^4 cells were cytospined on microscope slides (Knittel, Braunschweig) at 900 g for 1 min, using Cyto-Tek cytospin (Sakura, Hatfield, PA). The infection rate was assessed microscopically by counting the percentage of infected cells, after Giemsa staining (Merck, Darmstadt, Germany). IC_{50} values were calculated as described above.

2.3.3. Assessment of cytotoxicity in THP-1 monocytes

As a quantitative measurement of the cell damage, THP-1 cells at a density of 10^6/ml were incubated with serial dilutions of the compounds and their combinations, for 24 h at 37 °C/5% CO_2. Following incubation, cells were harvested, resuspended in PBS, stained with 12 μM PI, and analyzed by flow cytometry. Each compound was assigned the cytotoxic concentration CC_{50} (50% of maximum cytoxicity), calculated as described for the IC_{50} of promastigotes. Selectivity Index (SI) for each compound refers to the ratio CC_{50}/IC_{50} against the intracellular form.

2.3.4. Assessment of hemolytic potential

EDTA-preserved peripheral blood from healthy volunteers was centrifuged at 900 g for 10 min in order to remove serum, and washed three times in PBS. Red blood cells were distributed in 96-well microplates (Costar) and mixed equally with serial dilutions of the compounds and their combinations, at a ratio of 1:1 (v/v). Dilutions of the compounds were prepared in PBS. After incubation at 37 °C for 1 h, the plates were centrifuged at 900 g for 10 min and absorbance of the supernatants was measured at 550 nm, using Bio-Rad Microplate Reader Model 680 (Hercules, CA). HC_{50} values (Hemolytic concentration that causes 50% hemolysis) were calculated using the formula for the estimation of IC_{50}. Incubation of red blood cells with dH_2O was used for 100% hemolysis.

2.4. Synergistic effect of drug combinations

We have used the linear isobole approach introduced by Loewe and reviewed by Tallarida (2011). This is a graph in which the x axis are the doses of APCs that correspond to the IC_{50} for the intracellular amastigote when acting alone, and in the y axis are the corresponding doses of the peptaibols. The linear isobole is described by the equation a/A + b/B = 1, where A, B are the IC_{50} concentrations of the corresponding drugs and a,b are the theoretical doses of the two drugs that in combination produce the same effect as the individual IC_{50} effect. Each point on the isoboles represents the expected concentration of each one

of the components in the combination that will kill 50% of the intracellular parasites, when acting in a non-synergistic manner. If the intercept of the experimental concentrations of combined drugs plots off the line, this is an indication of drug interaction. When the drugs act synergistically the intercepts will plot below the line, whilst when they act antagonistically the intercepts will plot above the corresponding isobole.

The experimental data were produced by keeping constant the concentration of peptaibols and varying the concentration of APCs. More specifically, the percentage of infection of THP-1 cells was assessed at 24 h of treatment with linear dilutions of HePC (ranging from 15 μM to 0.2 μM), in the presence of 5 μM AAM or 2 μM SZ. Similarly, TC52 was used at concentrations ranging between 25 μM and 0.2 μM. The experimental doses a,b in the combination that produced the IC_{50} effect were plotted on the graph and used to quantify the Combination Index (CI) for each pair of drugs.

2.5. Effect on ROS production and mitochondrial membrane polarization

Promastigotes at a density of 5×10^5/ml were treated with the compounds and their combinations at the respective IC_{50} values. ROS production and mitochondrial membrane polarization were assessed at 1 h, 3 h and 6 h of incubation, using CM-H_2DCFDA and Mitotracker Red Dye (CMXRos), both obtained from Molecular Probes (Eugene, Oregon, USA), according to manufacturer's instructions. Briefly, pelleted promastigotes were incubated with 5 μM CM-H_2DCFDA for 30 min at 26 °C. Promastigotes were washed once with pre-warmed PBS, and further incubated at room temperature for 15 min to allow complete esterification of the diacetate groups. CM-H_2DCFDA is a cell-permeable non fluorescent probe which upon cleavage of its acetate groups by intracellular esterases and oxidation, yields a fluorescent adduct. Where appropriate, 0.1 μM Mitotracker was added and incubated for 30 min. Viability of promastigotes at 6 h of incubation was assessed by addition of 12 μM PI. Samples were immediately analyzed by flow cytometry as described below.

2.6. Flow cytometry analysis

Cell samples were analyzed using Cytomics FC500 flow cytometer (Beckman Coulter) equipped with a 488 nm laser. At least 10^4 cells were analyzed per sample. Data analysis was performed on fluorescence intensities that excluded cell auto-fluorescence and cell debris.

2.7. Morphological and ultrastuctural changes in promastigotes

For morphological analysis promastigotes were treated with HePC, AAM and their combination for 6 h at 26 °C, at concentrations that corresponded to the IC_{50} of each compound. Following incubation, parasites were harvested and washed twice in sodium cacodylate buffer (0.1 M SCB), by centrifugation at 300g for 10 min. Pellets were fixed with 2% glutaraldehyde (GDA)/2% paraformaldehyde (PFA) solution for 2 h and further processed for analysis with JEOL scanning electron microscope (JEOL, USA).

Ultrastuctural analysis was also performed with promastigotes that were treated with HePC, AAM and their combination for 6 h at 26 °C, at concentrations corresponding to the IC_{50}. Following incubation, promastigotes were harvested and washed twice in 0.1 M SCB by centrifugation at 300g for 10 min. Pellets were fixed with 2% GDA/2% PFA for 2 h and coated with 1% agar (Difco, BD, New Jersey). Coated pellets were further fixed by incubation with 2% GDA/2% PFA for 1 h, postfixed in 1% osmium tetroxide solution and embedded in epoxy resin. Ultrathin sections were analyzed with JEM-2100 transmission electron microscope (JEOL, USA).

Table 1
Biological activity of the compounds and their combinations.

Compound or combination	Intracellular amastigotes IC$_{50}$ (µM)[a]	CI[d]	Promastigotes IC$_{50}$ (µM)[b]	Cytotoxicity CC$_{50}$ (µM)[e]	Hemolysis HC$_{50}$(µM)[f]	% hemolysis[g]
HePC	1.8 ± 0.5		8.2 ± 0.7	28.6 ± 2.5	38.3 ± 2.8	96.1
TC52	6.6 ± 0.6		> 200	> 50	> 100	0.5
AAM	7.5 ± 0.2		8.7 ± 0.1	40.3 ± 3.2	94.6 ± 2.6	52.9
SZ	7.6 ± 1.2		8.2 ± 0.1	22.5 ± 3.2	66.9 ± 2.2	96.6
HePC/AAM[c]	0.3 ± 0.05	0.83				
HePC/SZ[c]	0.3 ± 0.06	0.43				
TC52/AAM[c]	1.4 ± 0.02	0.88				
TC52/2SZ[c]	2.5 ± 0.3	0.48				

[a,b] Drugs' activity referred as the 50% inhibitory concentration (IC$_{50}$) against the intracellular amastigote in THP-1 monocytes and promastigote form.

[c] Drug combinations' activity is referred as the IC$_{50}$ of the APC component that in the presence of stable peptaibol concentration (5 µM for AAM and 2 µM for SZ) killed 50% of the intracellular parasite.

[d] Combination Index (CI) values.

[e] Cytotoxicity is expressed as the 50% cytotoxic concentration (CC$_{50}$) against THP-1 monocytes.

[f] HC$_{50}$ is expressed as the compound concentration that yields 50% of the maximum hemolysis produced when human RBCs are incubated with water.

[g] % of hemolysis at 100 µM of each compound.

2.8. Statistical analysis

Data were collected from at least 3 different experiments, mean values and standard deviations were calculated and comparisons were made using Student's t-test. A P value < 0.05 was defined as significant.

3. Results

3.1. Evaluation of antileishmanial activity

The compounds were evaluated *in vitro* for their antileishmanial activity against the clinically relevant form of the parasite, the intracellular amastigote, as well as the promastigote form. The calculated IC$_{50}$ values for all compounds are shown in Table 1.

We used two different APC compounds, HePC and the synthetic analogue TC52 that although less active, has a therapeutic index higher than that of HePC (SI$_{TC52}$ > 75, SI$_{HePC}$:15.8). However, TC52 was inactive against promastigotes at the experimental concentrations used. Both peptaibols exhibited similar activity against the promastigote and the intracellular amastigote.

The antileishmanial activity of the combination of APCs with peptaibols against the intracellular amastigote form of the parasite was also assessed. For this purpose we used fixed doses of the peptaibols (5 µM of AAM and 2 µM of SZ) combined with variable concentrations of HePC or the analogue TC52. The above peptaibol concentrations were selected because they did not alter the cytotoxic or hemolytic effect of the phospholipids (Table 2). As shown in Table 1, the IC$_{50}$ value of HePC in combination with either of the peptaibols is 6-fold lower than the IC$_{50}$ value of HePC alone. Similarly, the IC$_{50}$ values of TC52 are 4.7-fold and

Table 2
Cytotoxicity and hemolytic activity of compounds and their combinations.

Compound or combination	% PI-stained THP-1 cells[a]	% Hemolysis[b]
HePC	27.6	8.8 ± 0.3
HePC/AAM	27.1	10.2 ± 0.6
HePC/SZ	31.4	9.4 ± 0.8
TC52	3.8	2.1 ± 0.1
TC52/AAM	3.8	1.5 ± 0.1
TC52/SZ	3	1.9 ± 0.2

Cytotoxic and hemolytic potential of 15 µM HePC and 25 µM TC52 combined with stable doses of 5 µM AAM and 2 µM SZ.

[a] Cytotoxic potential of drug combinations assessed by flow cytometry and expressed as % of PI positive cells.

[b] Hemolytic potential is expressed as % of hemolysis compared to the maximum hemolysis yielded when human RBCs are incubated with water.

2.6-fold lower when combined with AAM and SZ respectively.

3.2. Synergy between alkylphosphocholines and peptaibols

To investigate the possible synergistic leishmaniacidal effect of the APC/peptaibol combination, we have used the Loewe Additivity model, a widely employed model that classifies possible drug synergistic interactions in a stringent manner.

Based on the IC$_{50}$ of the drugs alone against the intracellular parasite, we have plotted the respective isoboles as described in Materials and Methods. Fig. 2 shows that the intercepts of the experimental dose pairs that kill 50% of the intracellular parasites plotted below the corresponding isoboles for both APCs, denoting an enhanced leishmanicidal activity due to a superadditive effect of the
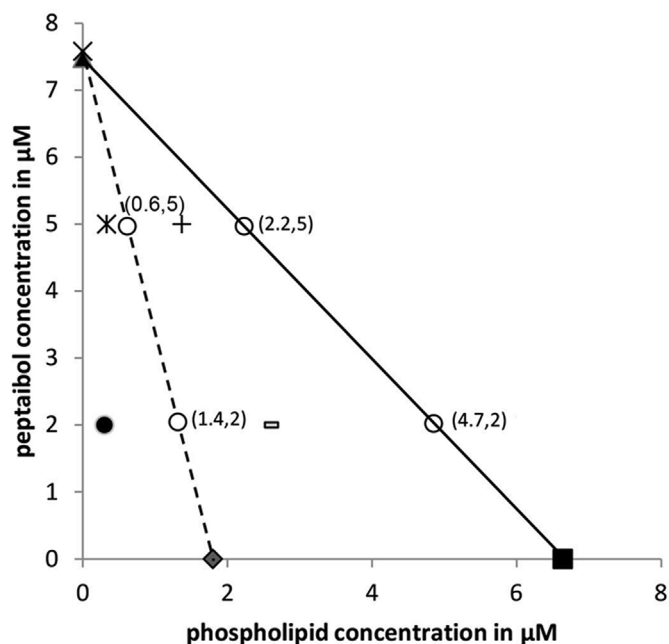

Fig. 2. Quantitative assessment of the combinatorial effect of the peptaibols AAM and SZ with the phospholipids HePC and TC52, based on the Loewe additivity model. Lines represent the defined isoboles limited by the IC$_{50}$ values of either peptaibols on the y axis and the IC$_{50}$ values of HePC (dashed line) and TC52 (solid line) in the x axis, respectively. Open circles represent the theoretical pairs of component doses that kill the 50% of the intracellular parasites in a simple additive manner. Experimental data of drug combinations: (∗) HePC/AAM, (●)HePC/SZ, (+)TC52/AAM, (·)TC52/SZ.

combinations.

Furthermore, the calculated CI values for all drug combinations were lower than 1 (Table 1), confirming the synergistic action of the compounds observed in the isobologram analysis. The combinations of both APCs with SZ exhibited lower CI values than those obtained with AAM, although the latter was used at higher concentration. More specifically, when HePC was combined with AAM or SZ, the respective CI values were 0.83 and 0.43. Similarly, when TC52 was combined with either AAM or SZ, the calculated CI values were 0.88 and 0.48 respectively.

3.3. Assessment of cytotoxic and hemolytic activity

The compounds were evaluated *in vitro* for their cytotoxicity against the human monocytic THP-1 cell line, also used for the determination of the antiparasitic activity on the intracellular stage of the parasite. Furthermore, their toxic effect on human red blood cells was assessed.

As shown in Table 1, the analogue TC52 was not cytotoxic against THP-1 cells, even at concentrations as high as 500 μM. Concerning peptaibols, AAM was about 1.8-fold less cytotoxic than SZ and 1.4-fold less cytotoxic than HePC. Similarly, the hemolytic potential of the peptaibols was lower than that of HePC (HC_{50} values 2.5-fold and 1.7-fold higher for AAM and SZ respectively).

The cytotoxic and hemolytic activity of the drug combinations was also assessed (Table 2). For this purpose the selected stable doses of 5 μM AAM and 2 μM SZ were used in combination with variable concentrations of the phospholipids. It was shown that at 15 μM HePC and 25 μM TC52 (which are the highest concentrations used for the determination of the antileishmanial activity against amastigotes), the cytotoxic and hemolytic potential of the combinations was comparable with the corresponding effect of the phospholipids alone.

3.4. Measurement of ROS levels

To determine the overall ROS production in promastigotes during incubation with the compounds we used the cell-permeable probe CM-H_2DCFDA. All compounds were used at concentrations corresponding to the IC_{50} and the percentage of ROS producing promastigotes was evaluated by flow cytometry (Fig. 3). Results showed that both AAM and SZ induced moderate levels of ROS that peaked at 6 h of treatment. Interestingly, both peptaibols when combined with HePC induced a
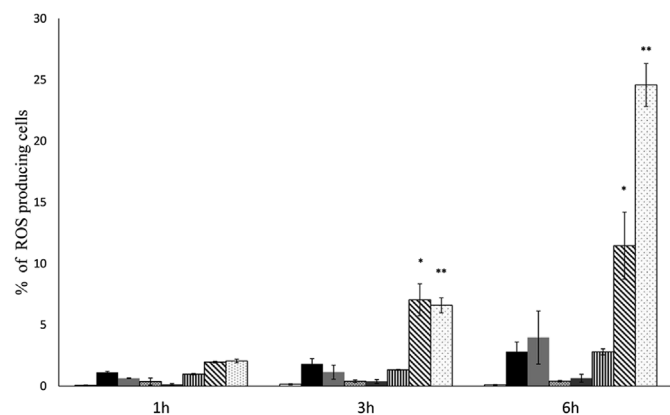
Fig. 3. Generation of ROS during treatment of promastigotes with the pepaibols, the phospholipids and their combinations. Data are expressed as percentage of ROS-producing promastigotes relative to control. Drugs and drug combinations: (☐) untreated, (∎) AAM, (▦) SZ, (▥) T52, (∎) HePC, (▥) AAM/TC52, (⊠) AAM/HePC, (☐) SZ/HePC. Values represent the mean ± SEM of at least 3 different experiments. * indicates significant difference of the AAM/HePC combination relative to AAM treated group (P < 0.05); ** indicates significant difference of the SZ/HePC combination relative to SZ treated group (P < 0.05).
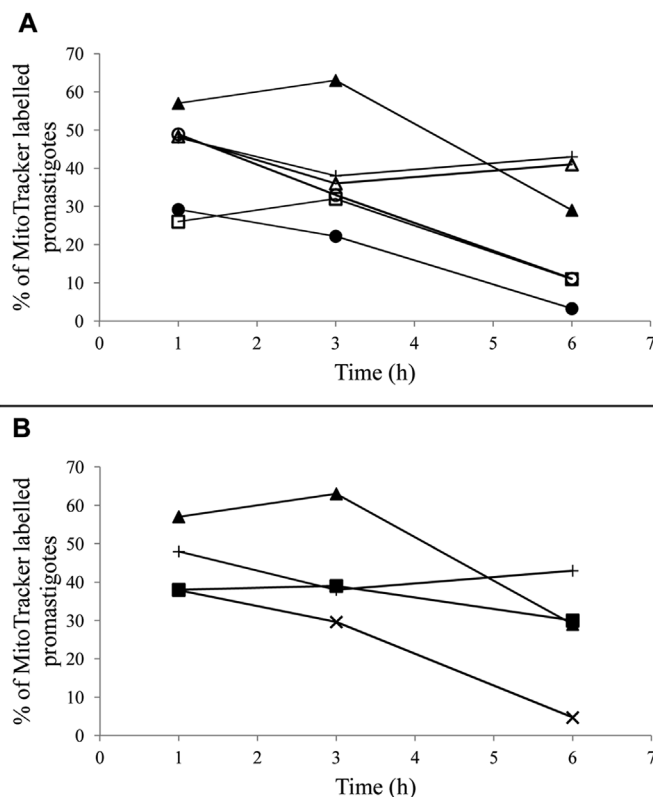
Fig. 4. MitoTracker retention in promastigotes treated with drugs and drug combinations. **A:** (+) untreated, (☐) AAM, (▲) HePC, (Δ) TC52, (○) AAM/TC52, (●) AAM/HePC. **B:** (+) untreated, (∎) SZ, (▲) HePC, (x) SZ/HePC. Data are expressed as percentage of promastigotes emitting fluorescence over 10^2 in the logarithmic scale at 630 nm, relative to control.

significant increase of ROS production at 3 h and 6 h of incubation, reaching a maximum after 6 h. ROS levels increased dramatically at 6 h of incubation in the combination of HePC/SZ. However, HePC induced low levels of ROS during the experiment, whereas the inactive TC52 did not influence the redox stage of promastigotes, as indicated by the absence of ROS production even at concentrations as high as 50 μM.

3.5. Evaluation of the alteration of mitochondrial physiology

Furthermore, we examined the status of the mitochondrial transmembrane potential, by staining of drug treated promastigotes with MitoTracker Red Dye (Fig. 4A and B). Although both peptaibols altered ΔΨm, AAM was able to inhibit mitochondrial function to a larger extent than SZ. Most importantly, we noticed that HePC was the only single-acting compound able to significantly induce accumulation of Mito-Tracker above the control levels, at 1 h and 3 h of treatment. However, when combined with peptaibols, mitochondria gradually lost their residual retention capacity and ΔΨm was completely collapsed after 6 h, indicating severe mitochondrial dysfunction. We noticed that the inactive TC52 did not influence mitochondrial function, since the observed effect of its combination with AAM was similar to the effect produced by the peptaibol alone.

3.6. Assessment of viability of promastigotes at early stages of treatment

The observed alterations on redox stage and mitochondrial physiology were correlated with viability of promastigotes at 6 h, after staining of treated cells with PI and flow cytometry analysis (Fig. 5). The effect of HePC on promastigote viability at 6 h was negligible (5.5% stained promastigotes compared to 4.4% in control), whereas it was increased by 5.3-fold and 2.2-fold in the presence of AAM and SZ
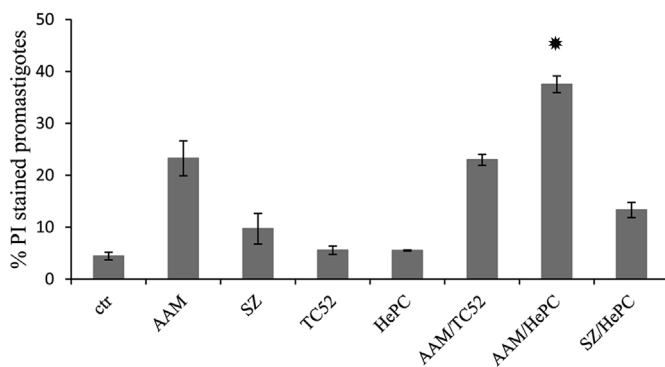
Fig. 5. Viability of promastigotes at 6 h of treatment with the peptaibols, the phospholipids and their combinations. Data are expressed as percentage of PI-stained promastigotes relative to control. Values represent the mean ± SEM of at least 3 different experiments. * indicates significant difference of the AAM/HePC combination relative to AAM treated group (P < 0.05).

respectively. However, only the combination AAM/HePC yielded a statistically significant increase in the percentage of PI-stained promastigotes, accompanied by an increase of the intracellular ROS levels, as well as reduction of $\Delta\Psi$m. Interestingly, the viability of promastigotes in the SZ/HePC combination was not affected at this time point, despite the marked increase in the production of intracellular ROS levels and $\Delta\Psi$m collapse, indicating that the two peptaibols influenced mitochondrial physiology in a different manner. However, the long term effect (24 h) of the above combinations on promastigote viability was comparable reaching 98% of PI positive cells. To notice that the combination of the inactive TC52 with AAM produced the same percentage of PI positive cells as AAM alone, at 6 h or at 24 h.

3.7. Morphological and ultrastructural observations

Scanning electron microscopy revealed morphological alterations in treated promastigotes, compared to untreated parasites that displayed normal morphology, with elongated shape and free flagellum. As shown in Fig. 6, treatment with AAM caused damage to the plasma membrane and altered flagellar morphology. These alterations were more pronounced in the AAM/HePC combination, although HePC itself did not seem to affect noticeably the morphology of parasites.

Transmission electron microscopy of treated promastigotes showed cytoplasmic vacuolization and ultrastructural alterations involving mainly mitochondria, that underwent significant morphological changes manifested by two distinct structural transformations. The phenotype of the AAM or AAM/HePC-treated promastigotes showed an imbalance in the fission/fusion process, leading to highly interconnected mitochondrial network or to bulky mitochondria (Fig. 6 C, D). These elongated and frequently branched structures adopted a curved shape around cytoplasmic material, resulting in either a closed "donut" structure (Fig. 6, Cc, arrow head) or an open ring structure with a pore not yet closed (Fig. 6, Cd, black arrow head). The morphology of the end-to-end (Fig. 6, Dd, black arrow heads) or side-to-end (Fig. 6, Cd, arrow head) mitochondria tethering complexes, bridged by membrane extensions, were frequently observed in the presence of AAM.

In HePC-treated cells mitochondria obtained mostly a rhabdoid or rounded configuration and, contrary to AAM-treated cells, the fission/fusion mechanism did not seem to be affected. The ring-like shape was the predominant morphology observed in HePC-treated samples, representing a vesicle-like structure. This structure seems to arise from the extension of mitochondrial membranes (Fig. 6, Bc and d, white arrows), that delimited an electronically sparse region resembling -cytoplasm (Fig. 6 B c white arrow head). It is worth noting that in some cells a budding vesicle-like ring is visible (Fig. 6, Bd, Cc, black arrows),

indicating that cristae participation in these structures could not be excluded.

4. Discussion

In our previous studies on structure-activity relationships of alkylphospholipids we described miltefosine derivatives substituted by rings of various sizes in the lipid portion and/or the head group, which have exhibited improved antileishmanial activity and reduced toxicity with respect to the prototype approved drug HePC (Avlonitis et al., 2003; Calogeropoulou et al., 2008; Papanastasiou et al., 2010; Godinho et al., 2013). APCs are a class of lipids that act directly or indirectly on the mitochondrion, resulting in alterations to membrane potential, leading to increased intracellular ROS levels and ultimately to cell death (Paris et al., 2004; Sen et al., 2004; Verma et al., 2007). Comparison of the effect on promastigotes of a number of APC analogues showed that the successful antileishmanial compounds including HePC, act on mitochondrial function during early stages of treatment (up to 6 h), by inducing mitochondrial swelling and transiently increasing $\Delta\psi$m (our unpublished data).

Synergistic drug combinations in treating infectious diseases exploit the chances for better efficacy, decreased toxicity and reduced development of drug resistance (Berg et al., 2015; Yadav et al., 2015). Our results showed that the two chemically different classes of compounds used, yielded a specific super-additive effect when combined against the intracellular clinical form of the parasite. However, the two peptaibols did not have an equivalent effect in the in vitro assay used. The 20-aa long SZ exhibited the highest additivity with both APCs, indicating that distinctive physicochemical characteristics influence the final synergistic outcome.

From a comparative study of the main structural and functional properties of selected peptaibols it has been shown that AAM and SZ-analogous alamethicin (Kirschbaum et al., 2003), a 16-residue and a 20-residue peptaibol respectively, form different channel types. It has been found that alamethicin, forms voltage-gated channels in planar lipid bilayers (Chugh and Wallace, 2001; Salnikov et al., 2009). At rest, without any applied voltage, the C-termini of alamethicin are assumed to aggregate as a layer on the membrane interface, whereas their N-termini bury into the lipid core to a different extent. Voltage increment results in increasing channel conductance, indicating that alamethicin molecules enter in the membrane, forming "barrel stave"-type channels in a voltage dependent manner. For AAM, the situation is likely to be quite different since its curved shape is predicted to favor significant embedment in the bilayer resulting in channel conductance, which is dependent on peptaibol concentration but not on voltage increment (Snook et al., 1998; Duclohier, 2004).

These findings could explain the behavior of the two peptaibols that we have assayed against promastigotes, specifically their effect on mitochondrial physiology. Looking at the early stages of treatment, AAM alone induced a transient increase of $\Delta\Psi$m at 3 h which was then dissipated by 75% of the control at 6 h, indicating that favorable conditions for conductive channel formation were achieved beyond 3 h of treatment, at the conditions tested. Conversely, in the absence of any stimulus that could influence $\Delta\Psi$m, SZ induced only mild effects during the first 6 h (30% $\Delta\Psi$m dissipation), indicating that no channel formation, able to influence mitochondrial function, was achieved under these conditions. The significant increase of $\Delta\Psi$m caused by HePC was probably the stimulus that enabled SZ to initiate channel formation, leading to the dramatic drop of $\Delta\Psi$m observed in the SZ/HePC combination.

In addition, the combination SZ/HePC induced the highest ROS levels that persisted, despite the loss of $\Delta\Psi$m, while AAM either alone or in combination with HePC, exerted a lower effect on the redox stage of the cell. Studies have shown that pore forming amphipathic peptides like alamethicin induce mitochondrial swelling that resembles the mitochondrial permeability transition pore. It was also found that
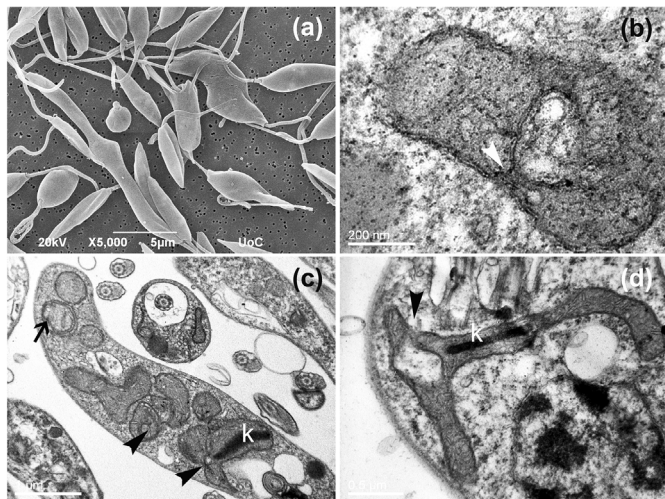
panel A
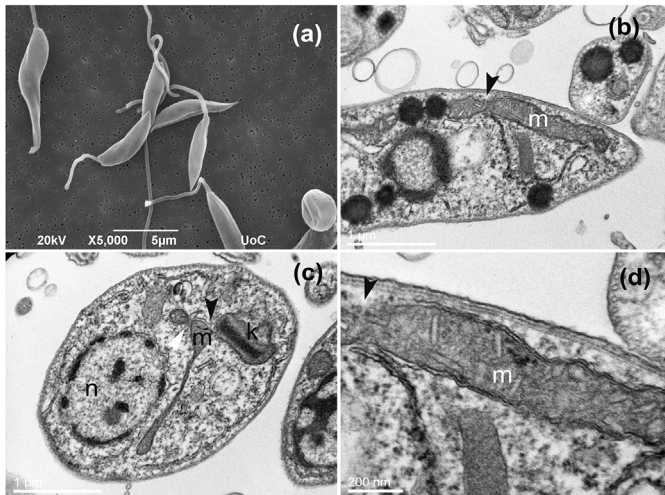
panel B
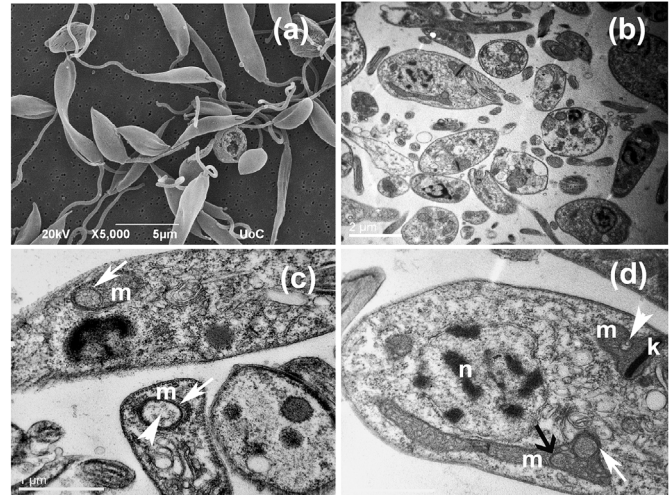
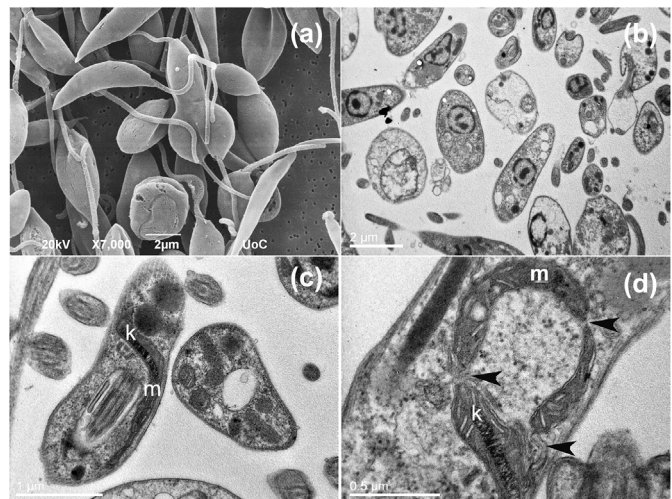**panel C**

panel D

Fig. 6. Morphological and ultrastructural alterations of *L. infantum* promastigotes after 6 h of treatment with AAM, HePC and their combination. **Panel A:** no treatment. **Panel B:** Mitochondria cristae remodeling and formation of co-centric membranes induced by HePC (Bc and Bd, white arrows). Rare appearance of spheroidal morphology (Bd, white arrow head). **Panel C:** AAM treatment induced plasma membrane injures (Ca) and promoted the formation of bulky curved mitochondria (Cb and Cd arrows). An interconnected mitochondrial network (Cc m) was formed in the majority of the cells. Spheroidal morphology of the mitochondria and cytoplasmic vacuolization was frequently observed. **Panel D:** Combination of AAM/HePC resulted to extensive damage of the plasma membrane (Da) and to extended inter-connection of mitochondria (Dd black arrow heads) with the characteristic curved structure.

alamethicin did not lead to complex I inhibition. Rather, the opposite happens, since permeabilization by alamethicin allows NADH to have access to its binding site on complex I, stimulating its activity (Hansson et al., 2008). This may be the explanation for high ROS generation, concomitant to the $\Delta\Psi$m loss observed in the presence of SZ: a functional complex I while ATP generation is abolished.

Along with disturbance of ROS and $\Delta\Psi$m, mitochondrial swelling and dysfunction can be stimulated by massive movement of Ca^{2+}, leading to mitochondrial Ca^{2+} imbalance (Jeyaraju et al., 2009). The channels formed by peptaibols are known to be cation permeable and they could act by facilitating the flux of ions towards the electrochemical gradient, deregulating Ca^{2+} handling between the cell compartments. The pore size able to support ion conductivity determines the concentration requirements and kinetics for $\Delta\Psi$m dissipation and cell death (Wilson et al., 2011). Both peptaibols need to reach a critical concentration in order to form cation permeable pores, for SZ however, as proposed for alamethicin (Kuang et al., 2014), increased

transmembrane voltage seems to be an extra requirement for pore stability.

In addition, the rate of pore forming capacity could not be attributed only to structural and functional properties of each peptaibol, but it could be influenced by the lipid composition of the membrane. Studies have shown that HePC modulates *Leishmania* metabolome after 3.75 h and many of the changes are related to short alkane production, potentially affecting the composition of cellular membranes (Vincent et al., 2014). Similarly, long treatment of *Leishmania* with low concentrations of HePC resulted in reduced phosphatidylcholine content and increased phosphatidylethanolamine percentage in membranes, altering membrane composition and possibly fluidity (Rakotomanga et al., 2007). Changes in membrane composition could act beneficially to channel formation capacity of peptaibols and consequently enhance their overall antileishmanial effect. As the synergistic effect appears to be a specific antileishmanial phenomenon, since no major toxic effect was observed on the host cell, we can conclude that the specific lipid

components of the parasite membranes may be the basis of the selective membranotoxic effect of the peptaibols.

Our results using the triazolyl-substituted miltefosine analogue TC52 enabled us to assess the possibility that the peptaibols could modulate the biological effect of an inert phosphocholine partner. However, when the inactive to promastigotes TC52 was combined with AAM no influence on mitochondrial function or the redox stage of promastigotes was observed. The only observed effect was the one exerted by the peptaibol. We thus suggest that the activity of the phosphocholine partner is a prerequisite to the final synergistic effect.

Our attention was attracted to the highly concatenated mitochondrial network and the spheroidal morphology of the mitochondria, observed after AAM treatment. The phenomenon is more prominent when the combination AAM/HePC was used, indicating that the specific biological effect on the mitochondrion caused by the peptide could be the foundation for this distinctive mitochondrial transformation. Spheroids are unique mitochondrial structures that could represent a common adaptation response to various mitochondrial stresses, including pharmacological ones (Christensen and Chapman, 1959; Stephens and Bils, 1965; Lauber, 1982; Ding et al., 2012b). Similar mitochondrial morphology can be observed in ultrastructural images of *L. amazonensis*, treated with 4-nitrobenzaldehyde thiosemicarbazone (Britta et al., 2014).

Although both morphological variants, the ring-like shape, promoted by HePC and the elongated bended mitochondria surrounding cytoplasmic content, induced by AAM, have been named collectively as spheroidal, it is not clear whether they represent the same subcellular phenomenon. In previous studies it was found that carbonyl cyanidem-chlorophe-nylhydrazone (CCCP), a reversible mitochondrial uncoupler, induced the spheroidal conformation in mammalian cells, in the absence of mitophagy triggering factors (Ding et al., 2012a). In that system the phenomenon was interpreted as an alternative to mitophagy response to stress signals, affected by ROS and the fusion-regulating proteins mitofusins. Although the role of mitofusins is not yet dissected in trypanosomatids, our observations evidenced a severe imbalance in the fission/fusion process as consequence of the AAM effect, independently of high ROS generation. The physiological role of spheroids as pro- or anti-apoptotic configurations remains however unclear and should be further investigated (Ding and Eskelinen, 2014; Williams and Ding, 2015).

5. Conclusion

Taken together, these results point towards the use of alternative treatments against leishmaniases, using synergistic drug combinations that present a great advantage over single compound therapies. The peptaibols AAM and the alamethicin-related SZ proved potent antileishmanial agents. They acted by destabilizing the mitochondrial membrane and induced extended mitochondrial morphological alterations. More importantly, they acted synergistically with APCs killing rapidly the intracellular parasite. The biological effects of AAM and SZ on promastigotes highlighted their distinctive mode of action and suggested that this huge family of amphipathic molecules could include members with distinguished anti-trypanosomatid features.

Funding

Conflicts of interest

None.

Acknowledgements

Appendix A. Supplementary data

Supplementary data related to this article can be found at http://dx.doi.org/10.1016/j.ijpddr.2018.03.005.

References

Ashby, M., Petkova, A., Hilpert, K., 2014. Cationic antimicrobial peptides as potential new therapeutic agents in neonates and children: a review. Curr. Opin. Infect. Dis. 27, 258–267.

Avlonitis, N., Lekka, E., Detsi, A., Koufaki, M., Calogeropoulou, T., Scoulica, E., Siapi, E., Kyrikou, I., Mavromoustakos, T., Tsotinis, A., Grdadolnik, S.G., Makriyannis, A., 2003. Antileishmanial ring-substituted ether phospholipids. J. Med. Chem. 46, 755–767.

Balaram, P., Krishna, K., Sukumar, M., Mellor, I.R., Sansom, M.S., 1992. The properties of ion channels formed by zervamicins. Eur. Biophys. J. 21, 117–128.

Berg, M., Garcia-Hernandez, R., Cuypers, B., Vanaerschot, M., Manzano, J.I., Poveda, J.A., Ferragut, J.A., Castanys, S., Dujardin, J.C., Gamarro, F., 2015. Experimental resistance to drug combinations in Leishmania donovani: metabolic and phenotypic adaptations. Antimicrob. Agents Chemother. 59, 2242–2255.

Berman, J., Bryceson, A.D., Croft, S., Engel, J., Gutteridge, W., Karbwang, J., Sindermann, H., Soto, J., Sundar, S., Urbina, J.A., 2006. Miltefosine: issues to be addressed in the future. Trans. R. Soc. Trop. Med. Hyg. 100 (Suppl. 1), S41–S44.

Boheim, G., 1974. Statistical analysis of alamethicin channels in black lipid membranes. J. Membr. Biol. 19, 277–303.

Britta, E.A., Scariot, D.B., Falzirolli, H., Ueda-Nakamura, T., Silva, C.C., Filho, B.P., Borsali, R., Nakamura, C.V., 2014. Cell death and ultrastructural alterations in Leishmania amazonensis caused by new compound 4-Nitrobenzaldehyde thiosemicarbazone derived from S-limonene. BMC Microbiol. 14, 236.

Bruckner, H., Graf, H., Bokel, M., 1984. Paracelsin; characterization by NMR spectroscopy and circular dichroism, and hemolytic properties of a peptaibol antibiotic from the cellulolytically active mold *Trichoderma reesei*. Part B. Experientia 40, 1189–1197.

Bruckner, H., Toniolo, C., 2013. Towards a myriad of peptaibiotics. Chem. Biodivers. 10, 731–733.

Calogeropoulou, T., Angelou, P., Detsi, A., Fragiadaki, I., Scoulica, E., 2008. Design and synthesis of potent antileishmanial cycloalkylidene-substituted ether phospholipid derivatives. J. Med. Chem. 51, 897–908.

Chappuis, F., Sundar, S., Hailu, A., Ghalib, H., Rijal, S., Peeling, R.W., Alvar, J., Boelaert, M., 2007. Visceral leishmaniasis: what are the needs for diagnosis, treatment and control? Nat. Rev. Microbiol. 5, 873–882.

Christensen, A.K., Chapman, G.B., 1959. Cup-shaped mitochondria in interstitial cells of the albino rat testis. Exp. Cell Res. 18, 576–579.

Chugh, J.K., Wallace, B.A., 2001. Peptaibols: models for ion channels. Biochem. Soc. Trans. 29, 565–570.

Croft, S.L., 2008. Kinetoplastida: new therapeutic strategies. Parasite 15, 522–527.

Croft, S.L., Barrett, M.P., Urbina, J.A., 2005. Chemotherapy of trypanosomiases and leishmaniasis. Trends Parasitol. 21, 508–512.

Croft, S.L., Neal, R.A., Pendergast, W., Chan, J.H., 1987. The activity of alkyl phosphorylcholines and related derivatives against Leishmania donovani. Biochem. Pharmacol. 36, 2633–2636.

David, C.V., Craft, N., 2009. Cutaneous and mucocutaneous leishmaniasis. Dermatol. Ther. 22, 491–502.

Desjeux, P., World Health Organization, Division of Control of Tropical Diseases, 1991. Information on the Epidemiology and Control of the Leishmaniases by Country or Territory. World Health Organization, Geneva.

Ding, W.X., Eskelinen, E.L., 2014. Do mitochondria donate membrane to form autophagosomes or undergo remodeling to form mitochondrial spheroids? Cell Biosci. 4, 65.

Ding, W.X., Guo, F., Ni, H.M., Bockus, A., Manley, S., Stolz, D.B., Eskelinen, E.L., Jaeschke, H., Yin, X.M., 2012a. Parkin and mitofusins reciprocally regulate mitophagy and mitochondrial spheroid formation. J. Biol. Chem. 287, 42379–42388.

Ding, W.X., Li, M., Biazik, J.M., Morgan, D.G., Guo, F., Ni, H.M., Goheen, M., Eskelinen, E.L., Yin, X.M., 2012b. Electron microscopic analysis of a spherical mitochondrial structure. J. Biol. Chem. 287, 42373–42378.

Dorlo, T.P., Balasegaram, M., Beijnen, J.H., de Vries, P.J., 2012. Miltefosine: a review of its pharmacology and therapeutic efficacy in the treatment of leishmaniasis. J. Antimicrob. Chemother. 67, 2576–2597.

Duclohier, H., 2004. Helical kink and channel behaviour: a comparative study with the peptaibols alamethicin, trichotoxin and antiamoebin. Eur. Biophys. J. 33, 169–174.

Gaidukov, L., Fish, A., Mor, A., 2003. Analysis of membrane-binding properties of dermaseptin analogues: relationships between binding and cytotoxicity. Biochemistry

42, 12866–12874.

Godinho, J.L., Georgikopoulou, K., Calogeropoulou, T., de, S.W., Rodrigues, J.C., 2013. A novel alkyl phosphocholine-dinitroaniline hybrid molecule exhibits biological activity in vitro against Leishmania amazonensis. Exp. Parasitol. 135, 153–165.

Guerrero, E., Saugar, J.M., Matsuzaki, K., Rivas, L., 2004. Role of positional hydrophobicity in the leishmanicidal activity of magainin 2. Antimicrob. Agents Chemother. 48, 2980–2986.

Hancock, R.E., Diamond, G., 2000. The role of cationic antimicrobial peptides in innate host defences. Trends Microbiol. 8, 402–410.

Hansson, M.J., Mansson, R., Morota, S., Uchino, H., Kallur, T., Sumi, T., Ishii, N., Shimazu, M., Keep, M.F., Jegorov, A., Elmer, E., 2008. Calcium-induced generation of reactive oxygen species in brain mitochondria is mediated by permeability transition. Free Radic. Biol. Med. 45, 284–294.

Herwaldt, B.L., 1999. Miltefosine–the long-awaited therapy for visceral leishmaniasis? N. Engl. J. Med. 341, 1840–1842.

Huber, W., Koella, J.C., 1993. A comparison of three methods of estimating EC50 in studies of drug resistance of malaria parasites. Acta Trop. 55, 257–261.

Jaworski, A., Bruckner, H., 2000. New sequences and new fungal producers of peptaibol antibiotics antiamoebins. J. Pept. Sci. 6, 149–167.

Jeyaraju, D.V., Cisbani, G., Pellegrini, L., 2009. Calcium regulation of mitochondria motility and morphology. Biochim. Biophys. Acta 1787, 1363–1373.

Kirschbaum, J., Krause, C., Winzheimer, R.K., Bruckner, H., 2003. Sequences of ala-methicins F30 and F50 reconsidered and reconciled. J. Pept. Sci. 9, 799–809.

Krause, C., Kirschbaum, J., Jung, G., Bruckner, H., 2006. Sequence diversity of the peptaibol antibiotic suzukacillin-A from the mold Trichoderma viride. J. Pept. Sci. 12, 321–327.

Kuang, Q., Purhonen, P., Jegerschold, C., Hebert, H., 2014. The projection structure of Kch, a putative potassium channel in Escherichia coli, by electron crystallography. Biochim. Biophys. Acta 1838, 237–243.

Kulkarni, M.M., McMaster, W.R., Kamysz, E., Kamysz, W., Engman, D.M., McGwire, B.S., 2006. The major surface-metalloprotease of the parasitic protozoan, Leishmania, protects against antimicrobial peptide-induced apoptotic killing. Mol. Microbiol. 62, 1484–1497.

Kumar, A., Dhuley, J.N., Naik, S.R., 1991. Evaluation of microbial metabolites for trypanocidal activity: significance of biochemical and biological parameters in the mouse model of trypanosomiasis. Jpn. J. Med. Sci. Biol. 44, 7–16.

Lauber, J.K., 1982. Retinal pigment epithelium: ring mitochondria and lesions induced by continuous light. Curr. Eye Res. 2, 855–862.

Lira, R., Contreras, L.M., Rita, R.M., Urbina, J.A., 2001. Mechanism of action of antiproliferative lysophospholipid analogues against the protozoan parasite Trypanosoma cruzi: potentiation of in vitro activity by the sterol biosynthesis inhibitor ketoconazole. J. Antimicrob. Chemother. 47, 537–546.

Lux, H., Hart, D.T., Parker, P.J., Klenner, T., 1996. Ether lipid metabolism, GPI anchor biosynthesis, and signal transduction are putative targets for anti-leishmanial alkyl phospholipid analogues. Adv. Exp. Med. Biol. 416, 201–211.

Mangoni, M.L., Saugar, J.M., Dellisanti, M., Barra, D., Simmaco, M., Rivas, L., 2005. Temporins, small antimicrobial peptides with leishmanicidal activity. J. Biol. Chem. 280, 984–990.

Matha, V., Jegorov, A., Kiess, M., Bruckner, H., 1992. Morphological alterations accompanying the effect of peptaibiotics, alpha-aminoisobutyric acid-rich secondary metabolites of filamentous fungi, on Culex pipiens larvae. Tissue Cell 24, 559–564.

Mishra, J., Saxena, A., Singh, S., 2007. Chemotherapy of leishmaniasis: past, present and future. Curr. Med. Chem. 14, 1153–1169.

Murray, M., Dyari, H.R., Allison, S.E., Rawling, T., 2014. Lipid analogues as potential drugs for the regulation of mitochondrial cell death. Br. J. Pharmacol. 171, 2051–2066.

Nagaraj, G., Uma, M.V., Shivayogi, M.S., Balaram, H., 2001. Antimalarial activities of peptide antibiotics isolated from fungi. Antimicrob. Agents Chemother. 45, 145–149.

Papanastasiou, I., Prousis, K.C., Georgikopoulou, K., Pavlidis, T., Scoulica, E., Kolocouris,

N., Calogeropoulou, T., 2010. Design and synthesis of new adamantyl-substituted antileishmanial ether phospholipids. Bioorg. Med. Chem. Lett 20, 5484–5487.

Paris, C., Loiseau, P.M., Bories, C., Breard, J., 2004. Miltefosine induces apoptosis-like death in Leishmania donovani promastigotes. Antimicrob. Agents Chemother. 48, 852–859.

Peltola, J., Ritieni, A., Mikkola, R., Grigoriev, P.A., Pocsfalvi, G., Andersson, M.A., Salkinoja-Salonen, M.S., 2004. Biological effects of Trichoderma harzianum peptaibols on mammalian cells. Appl. Environ. Microbiol. 70, 4996–5004.

Rakotomanga, M., Blanc, S., Gaudin, K., Chaminade, P., Loiseau, P.M., 2007. Miltefosine affects lipid metabolism in Leishmania donovani promastigotes. Antimicrob. Agents Chemother. 51, 1425–1430.

Reed, P.W., Lardy, H.A., 1975. Uncoupling, and specific inhibition of phosphoryl transfer reactions in mitochondria by antibiotic A20668. J. Biol. Chem. 250, 3704–3708.

Salnikov, E.S., Friedrich, H., Li, X., Bertani, P., Reissmann, S., Hertweck, C., O'Neil, J.D., Raap, J., Bechinger, B., 2009. Structure and alignment of the membrane-associated peptaibols ampullosporin A and alamethicin by oriented 15N and 31P solid-state NMR spectroscopy. Biophys. J. 96, 86–100.

Santa-Rita, R.M., Henriques-Pons, A., Barbosa, H.S., de Castro, S.L., 2004. Effect of the lysophospholipid analogues edelfosine, ilmofosine and miltefosine against Leishmania amazonensis. J. Antimicrob. Chemother. 54, 704–710.

Sen, N., Das, B.B., Ganguly, A., Mukherjee, T., Bandyopadhyay, S., Majumder, H.K., 2004. Camptothecin-induced imbalance in intracellular cation homeostasis regulates programmed cell death in unicellular hemoflagellate Leishmania donovani. J. Biol. Chem. 279, 52366–52375.

Shi, M., Wang, H.N., Xie, S.T., Luo, Y., Sun, C.Y., Chen, X.L., Zhang, Y.Z., 2010. Antimicrobial peptaibols, novel suppressors of tumor cells, targeted calcium-mediated apoptosis and autophagy in human hepatocellular carcinoma cells. Mol. Canc. 9, 26.

Sindermann, H., Engel, K.R., Fischer, C., Bommer, W., 2004. Oral miltefosine for leishmaniasis in immunocompromised patients: compassionate use in 39 patients with HIV infection. Clin. Infect. Dis. 39, 1520–1523.

Snook, C.F., Woolley, G.A., Oliva, G., Pattabhi, V., Wood, S.F., Blundell, T.L., Wallace, B.A., 1998. The structure and function of antiamoebin I, a proline-rich membrane-active polypeptide. Structure 6, 783–792.

Stephens, R.J., Bils, R.F., 1965. An atypical mitochondrial form in normal rat liver. J. Cell Biol. 24, 500–504.

Szekeres, A., Leitgeb, B., Kredics, L., Antal, Z., Hatvani, L., Manczinger, L., Vagvolgyi, C., 2005. Peptaibols and related peptaibiotics of Trichoderma. A review. Acta Microbiol. Immunol. Hung. 52, 137–168.

Tallarida, R.J., 2011. Quantitative methods for assessing drug synergism. Gene Canc. 2, 1003–1008.

Teixeira, V., Feio, M.J., Bastos, M., 2012. Role of lipids in the interaction of antimicrobial peptides with membranes. Prog. Lipid Res. 51, 149–177.

Verma, N.K., Singh, G., Dey, C.S., 2007. Miltefosine induces apoptosis in arsenite-resistant Leishmania donovani promastigotes through mitochondrial dysfunction. Exp. Parasitol. 116, 1–13.

Vincent, I.M., Weidt, S., Rivas, L., Burgess, K., Smith, T.K., Ouellette, M., 2014. Untargeted metabolomic analysis of miltefosine action in Leishmania infantum reveals changes to the internal lipid metabolism. Int. J. Parasitol. Drugs Drug Resist. 4, 20–27.

Williams, J.A., Ding, W.X., 2015. Mitophagy, mitochondrial spheroids, and mitochondrial-derived vesicles in alcohol-induced liver injury. Am. J. Physiol. Gastrointest. Liver Physiol. 309, G515.

Wilson, M.A., Wei, C., Bjelkmar, P., Wallace, B.A., Pohorille, A., 2011. Molecular dynamics simulation of the antiamoebin ion channel: linking structure and conductance. Biophys. J. 100, 2394–2402.

Yadav, B., Wennerberg, K., Aittokallio, T., Tang, J., 2015. Searching for drug synergy in complex dose-response landscapes using an interaction potency model. Comput. Struct. Biotechnol. J. 13, 504–513.